Accepted Manuscript

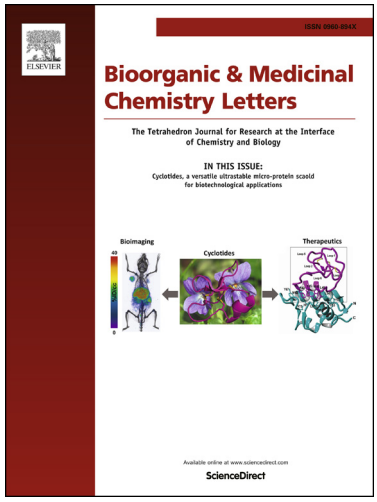

Indole Acids as a Novel PDE2 Inhibitor Chemotype that Demonstrate Pro-Cognitive Activity in Multiple Species

Shawn J. Stachel, Melissa S. Egbertson, Jenny Wai, Michelle Machacek, Dawn M. Toolan, John Swestock, Donnie M. Eddins, Vanita Puri, Georgia McGaughey, Hua-Poo Su, Debbie Perlow, Deping Wang, Lei Ma, Gopal Parthasarathy, John C. Reid, Pravien D. Abeywickrema, Sean M. Smith, Jason M. Uslaner

PII: S0960-894X(18)30049-0
DOI: https://doi.org/10.1016/j.bmcl.2018.01.039
Reference: BMCL 25565

To appear in: *Bioorganic & Medicinal Chemistry Letters*

Received Date: 14 November 2017
Revised Date: 19 January 2018
Accepted Date: 20 January 2018

Please cite this article as: Stachel, S.J., Egbertson, M.S., Wai, J., Machacek, M., Toolan, D.M., Swestock, J., Eddins, D.M., Puri, V., McGaughey, G., Su, H-P., Perlow, D., Wang, D., Ma, L., Parthasarathy, G., Reid, J.C., Abeywickrema, P.D., Smith, S.M., Uslaner, J.M., Indole Acids as a Novel PDE2 Inhibitor Chemotype that Demonstrate Pro-Cognitive Activity in Multiple Species, *Bioorganic & Medicinal Chemistry Letters* (2018), doi: https://doi.org/10.1016/j.bmcl.2018.01.039

Indole Acids as a Novel PDE2 Inhibitor Chemotype that Demonstrate Pro-Cognitive Activity in Multiple Species

Shawn J. Stachel,[a] Melissa S. Egbertson,[a] Jenny Wai,[a] Michelle Machacek,[a] Dawn M. Toolan,[d] John Swestock,[a] Donnie M. Eddins,[b] Vanita Puri,[b] Georgia McGaughey,[c] Hua-Poo Su,[c] Debbie Perlow,[a] Deping Wang,[c] Lei Ma,[d] Gopal Parthasarathy,[c] John C. Reid,[c] Pravien D. Abeywickrema,[c] Sean M. Smith,[d] Jason M. Uslaner[d]

[a] *Department of Medicinal Chemistry, Merck & Co. Inc., PO Box 4, West Point, PA 19486, USA*

[b] *Department of pharmacology Merck & Co. Inc., PO Box 4, West Point, PA 19486, USA*

[c] *Department of Structural Biology, Merck & Co. Inc, PO Box 4, West Point, PA 19486, USA*

[d] *Department of Neuroscience, Merck & Co. Inc., PO Box 4, West Point, PA 19486, USA*

This is where the receipt/accepted dates will go; Received Month XX, 2000; Accepted Month XX, 2000 [BMCL RECEIPT]

Abstract— An internal HTS effort identified a novel PDE2 inhibitor series that was subsequently optimized for improved PDE2 activity and off-target selectivity. The optimized lead, compound **4**, improved cognitive performance in a rodent novel object recognition task as well as a non-human primate object retrieval task. In addition, co-crystallization studies of close analog of 4 in the PDE2 active site revealed unique binding interactions influencing the high PDE isoform selectivity.

Schizophrenia is a debilitating disorder typically diagnosed in individuals in their early to mid-twenties. There are multiple symptoms, which are typically clustered into so-called positive, negative, and cognitive symptoms. Currently available therapies improve the positive symptoms, such as hallucinations and aggression, but tend not to affect negative symptoms such as anhedonia, or the cognitive symptoms such as memory and executive function deficits. Several investigations have shown that cognitive dysfunction is most predictive of every day function,[1] and for this reason a significant amount of research has been aimed at identifying new mechanisms to treat cognitive disturbances associated with schizophrenia. Unfortunately, this is still an unmet medical need.

In an effort to identify novel treatments for cognitive impairment associated with schizophrenia, we focused on targets that could modulate the second messengers cyclic guanosine monophosphate (cGMP) and cyclic adenosine monophosphate (cAMP). These ubiquitous secondary messengers are responsible for altering the function of many intracellular proteins, are involved in synaptic plasticity such as long-term potentiation, and are downstream signaling molecules of dopamine and glutamate, two neurotransmitters believed to be altered in the disease. One strategy for affecting the levels of these cyclic nucleotides is to inhibit 3', 5'-cyclic nucleotide specific phosphodiesterases (PDEs), which are a group of enzymes that degrade these secondary messengers. The PDE superfamily includes twenty-one genes that encode for eleven families of PDEs. These

families are further subdivided based on catalytic domain homology and substrate specificity and include: cAMP specific, PDE4A-D, 7A and 7B, and 8A and 8B; cGMP specific, PDE 5A, 6A-C, and 9A; and dual substrate, PDE 1A-C, 2A, 3A and 3B, 10A, and 11A. The homology between the families, ranging from 20% to 45%, suggests that it may be possible to develop selective inhibitors for each of these families.

Inhibition of PDE2 has been shown to enhance cognitive function in multiple rodent assays of cognitive performance measuring recognition memory, social interactions and working memory, which are all deficient in schizophrenia.[2] However, as far as we know, the effect of PDE2 inhibitors on cognitive function in non-human primate, which might be a better model of human cognition, has not been demonstrated. Our efforts described here were aimed at identifying a compound with suitable properties to evaluate the cognitive effects of PDE2 inhibition in non-human primate.

As part of our internal effort to identify novel PDE2 inhibitors we embarked on an HTS campaign as well as a fragment screening effort. The HTS screen yielded a variety of potent hits. In particular, compounds of the indole class represented by **1** demonstrated good potency and pharmacokinetic properties to serve as a starting point for series optimization (Figure 1). This class of compounds had been previously explored by us as part of the prostanoid receptor antagonist program culminating in the Phase II clinical candidate Laropiprant, **2**, a selective prostaglandin DP1 receptor antagonist that reduces the vasodilation and flushing induced by niacin therapy.[3,4] Compound **1** displayed good PDE2 inhibitory activity as a screening hit (PDE2, IC_{50} = 95 nM) and high PDE isoform selectivity with selectivities for $PDE_{3\text{-}11}$ > 1000-fold with the lowest selectivity being for PDE_1 at 124-fold. Unfortunately **1** still retained significant intrinsic activity as a DP1 antagonist, with a DP1 IC_{50} = 4 nM, that would need to be address to advance the series.

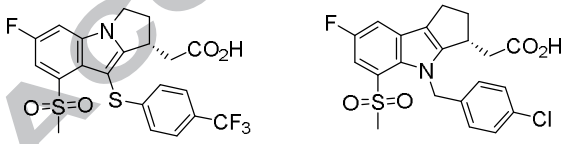

Figure 1. HTS lead and subsequent benchmark compound **1**.

As observed from the historical prostanoid program the *R* stereochemistry for the acetic acid functional group is preferred for DP1 potency in compound **1**. Inversion of the indole acid side chain stereochemistry from the *R* to the *S* configuration as present in compound **3**, Figure 2, was found to reduce the potency for DP1 while having negligible effect on PDE2 potency. Next it was discovered that expansion of the the fused five-membered ring system to a six-membered ring (**4**) enhanced PDE2 potency ~ 3-fold and also decreased DP1 activity 3-fold between the two systems thus improving the PDE2/DP1 selectivity from 2-fold to 25-fold. Compound **4** also retained its high selectivity profile against the other PDEs, *i.e*. 3-11, but now included the previous deficient PDE1 with >1000-fold selectivity versus PDE isoforms 1-11.

As such, compound **4** was profiled in vivo in rats and displayed pharmacokinetic properties supportive of in vivo pharmacodynamic studies (Cl = 19 mL/min/kg; $t_{1/2}$ = 4.7 h; V_{dss} = 3.6 L/kg; %F = 30%; rat PPB = 98%).

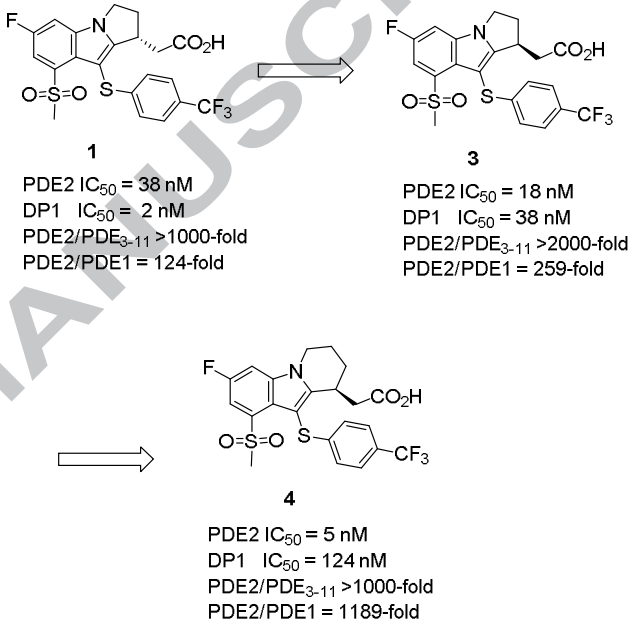

Figure 2. Elaboration of indole hit **1**.

Possessing sufficient potency, isoform selectivity, and pharmacokinetic properties, compound **4** was subsequently evaluated for its ability to improve recognition memory as assayed in the novel object recognition test. This task consisted of exposing vehicle- or scopolamine-treated rats to two identical objects and then exposing the rats 1h later to one object they had previously been exposed to and one object that was novel. Animals not administered scopolamine will spend more time exploring a novel object than a familiar one, indicating that they recognize the object they had been exposed to. Administration of scopolamine, however, impairs recognition memory such that animals will explore both the familiar and novel object approximately equally. The red dashed line in Figure 3 represents the 50% mark, or equivalent time exploring the novel and familiar objects. As seen in Figure 3, compound **4** dose-dependently increased novel object exploration at the 1 and 3 mg/kg dose levels by ~15%, and pharmacokinetic studies indicate

that these doses produce exposures corresponding to unbound compound levels in plasma equivalent to 1 and 2-fold over the IC_{50} value observed in the biochemical PDE2 assay. The effect seen at these doses was comparable to the effect of donepezil which is used as the gold standard comparator in the assay. An inverted U-shaped response was observed with reduced efficacy at the higher dose levels, an effect often observed with pre-clinical cognitive function and memory assays.[5]

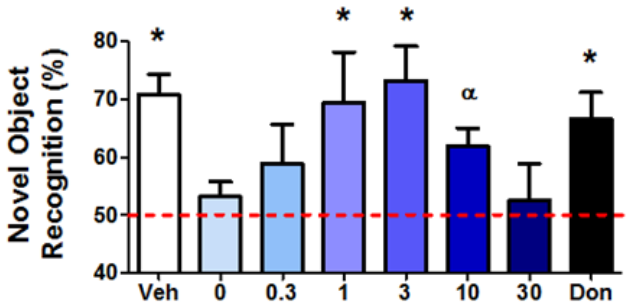

Dose (mg/kg)	Plasma (μM)	Free cmpd (μM)
0.3	0.051	0.001
1.0	0.205	0.005
3.0	0.413	0.010

Figure 3. Rat Novel Object Recognition study with compound **4**

Compound **4** was also tested in a non-human primate model of executive function, the rhesus object retrieval assay.[6,7] As was seen in the rodent novel object recognition study, statistically significant reversal of the scopolamine impairment was observed at the 1 and 3 mg/kg doses, equating to 2 and 10-fold unbound plasma concentration as a measure of fold over the biochemical IC_{50} value.

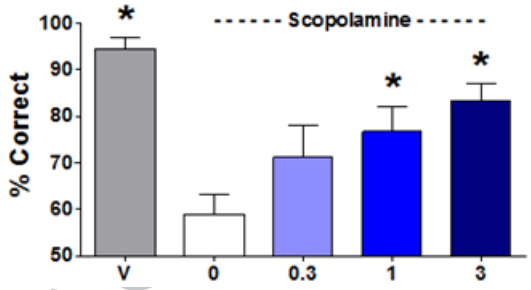

Dose (mg/kg)	Plasma (μM)	Free cmpd (μM)
0.3	0.137	0.004
1.0	0.439	0.013
3.0	1.598	0.048
5.0	2.976	0.089

Figure 4. Effects on Object Retrieval in Scopolamine-Impaired Adult Rhesus Monkeys with compound **4**.

Compound **4** and similar analogs were conveniently prepared as depicted in Scheme 1.[3,8] The synthesis begins with conversion of methyl 2-bromoacetate (**5**) to the corresponding azide (**6**). An aldol condensation of compound **6** with 2-bromo-4-fluorobenzaldehyde yielded the α,β-unsaturated azido ester **7** which upon thermolysis afforded indole ester **8**. Alkylation of **8** with 4-bromobutanoate followed by Dieckmann condensation resulted in formation of the β-keto ester that was decarboxylated under acidic conditions to produce ketone **9**. Ketone **9** was stereoselectively reduced using Corey-Bakshi-Shibata conditions with the chiral oxaborolidine *R*-CBS reagent to give the *S*-alcohol.[9] The chiral alcohol was then elaborated to the homologated ester **10** by activation of the alcohol as the phosphate which was displaced by dimethyl malonate and after subsequent decarboxylation afforded intermediate **10**. The thioaryl group was then installed by treatment of **10** with 1,2-bis-(4-(trifluoromethyl)phenyldisulfane after which hydrolysis of the ester afforded the desired acid **4**.

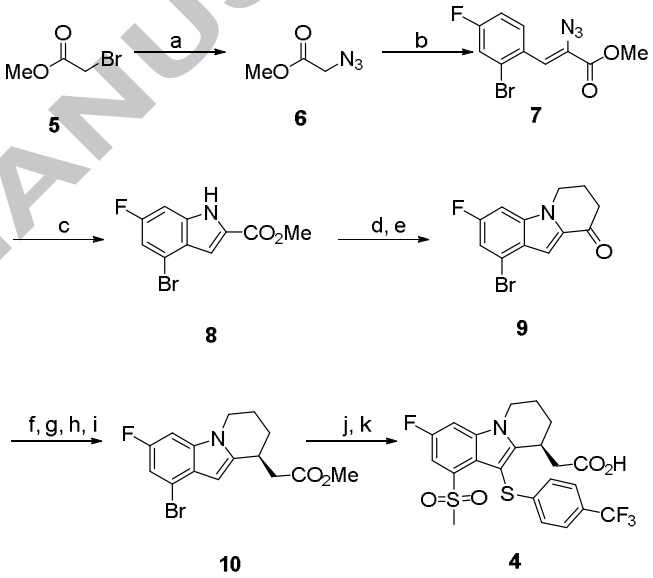

Reagents and conditions: (a) NaN_3, MeOH:H_20 (b) 2-Bromo-4-fluorobenzaldehyde, NaOMe, MeOH (c) xylenes, heat (d) NaH, methyl 4-bromobutanoate, TBAI, DMF e) HCl, EtOH (f) (*R*) CBS, CH_2Cl_2 BH_3-DMS, -30°C (g) NaHMDS, $(PhO)_2POCl$, -78°C (h) dimethyl malonate, NaHMDS, -78°C (i) NaCl, DMSO, H_20, 150°C 20 h (j) 1,2-bis(4-(trifluoromethyl)phenyl)disulfane, DCE, DMF, 0°C - RT (k) LiOH, THF:MeOH 50°C

Scheme 1: Synthetic route for compound **4**.

Although compound **4** displayed several favorable attributes such as good PDE2 potency, high isoform selectivity and a positive in vivo pharmacodynamic effect we still sought to further reduce the inherent DP1 activity of the series. This was achieved by reversing the position on the indole nitrogen from a tetrahydropyrido-indole scaffold in **4** to a tetrahydrocarbazole scaffold as shown in compound **11**. The carbazole scaffold also allowed for facile introduction of a chiral carbon atom to replace the sulfur

atom in the tetrahydropyrido-indole scaffold. This modification resulted in compounds that retained PDE2 activity while improving the selectivity versus the DP1 with compound **11** now exhibiting 100-fold selectivity over DP1.

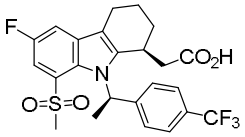

11

PDE2 IC_{50} = 7 nM
DP1 Ki = 674 nM

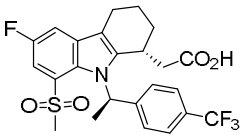

12

PDE2 IC_{50} = 1548 nM
DP1 IC_{50} = 13 nM

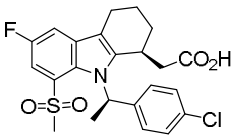

13

PDE2 IC_{50} = 31 nM
DP1 Ki = 873 uM

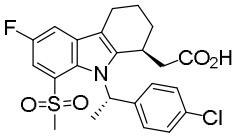

14

PDE2 IC_{50} = 3465 nM
DP1 IC_{50} = 17 nM

Figure 5. SAR in tetrahydrocarbazole series.

While the *R* stereochemistry at the acetic acid position has been shown to be a slightly favored for PDE2 activity and DP1 selectivity in the tetrahydropyrido-indole scaffold as seen in compounds **1** and **3** it was a more critical determinant for both PDE2 potency and selectivity over DP1 in the tetrahydrocarbazole series as depicted in compounds **11** and **12**. Interesting, in addition to the lower PDE2 activity for the *S* compound **12**, there was also a severe degradation in the PDE isoform selectivity with this isomer as well (data not shown). Another notable observation was that inversion of the stereochemistry at the benzyl center was also capable of reversing the PDE potency and DP1 selectivity profile even with the preferred *R*-acetic acid stereoisomer as depicted by compounds **13** and **14**.

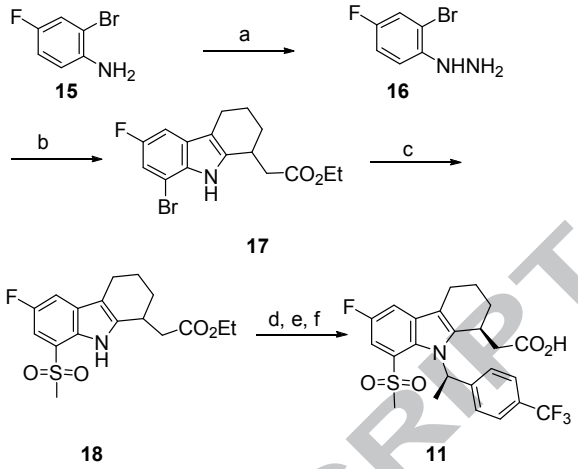

15 **16** **17** **18** **11**

Reagents and conditions: a) i) HCl, $NaNO_2$ ii) $SnCl_2$, 83% b) HOAc, 120°C, 35%c) $MeSO_3Na$, CuI, 60% d) DIAD, triphenylphosphine, toluene 20% e) chiral seperation f) LiOH, THF: MeOH 90%

Scheme 2. Synthetic scheme for compound **11**.

Compound **11** was conveniently prepared prepared using a Fischer-Indole route as depicted in Scheme 2.[10,11] 2-bromo-4-fluoroaniline (**15**) was converted to the corresponding hydrazine (**16**) using sodium nitrate. Hydrazine **16** was used for a Fischer-Indole reaction with ethyl 2-(2-oxocyclohexyl)acetate to provide tetrahydrocarbazole **17**. The bromide of the tetrahydrocarbazole was then converted to the methylsulfone and using sodium methane sulfonate and copper iodide to yield compound **18**. A Mitsunobu reaction with (*S*)-1-(4-(trifluoromethyl)phenyl)ethan-1-ol was then employed to install the benzyl group on the indole nitrogen with defined stereochemistry. Finally, chiral HPLC separation at the ester stage followed by hydrolysis to the corresponding acid produced **11** in good overall yield.

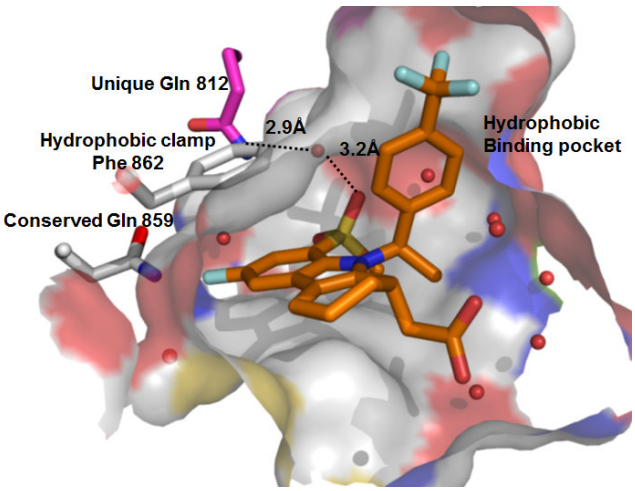

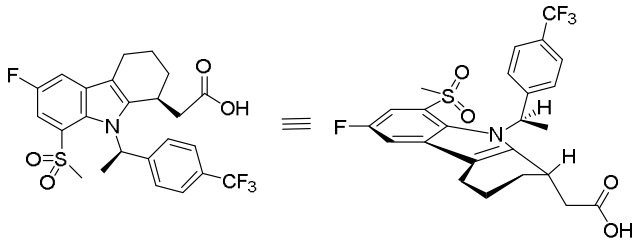

Figure 6. X-ray crystal structure of **11** bound in the PDE2 catalytic site (PDB 6BLF).[12]

Gratifyingly, the X-ray structure of **11** bound in the PDE2 catalytic site was solved and revealed several noteworthy interactions. As shown in Figure 6, the aromatic ring of the indole is anchored in the cAMP binding pocket through a face-face π-stacking interaction with Phe862 and an edge-to-face π-stacking interaction with Phe830, these interactions are commonly referred to in PDE nomenclature as the hydrophobic clamp region. There is also unique hydrogen-bonding interaction between Gln859, which is conserved in most PDEs, and the fluorine atom present in **11**. The para-CF_3 benzyl group is situated in a binding-induced hydrophobic pocket between Ile866 and Leu770 which is unique to PDE2 and has been described in earlier publications.[13] The structure also showed compound **11** involved in a water-mediated hydrogen bond between one of the oxygen atoms on the sulfone and residue Gln812, a residue unique to PDE2. Interactions with Gln812 and occupation of the hydrophobic binding pocket likely lead to the high PDE isoform selectivity of this series. Finally, the acetic acid group is involved with two water-mediated hydrogen bonds, one to the NH of Leu770 one to the NH of Asn705. In addition to the two water-mediated hydrogen bonds the acetic acid functionality is also involved with a direct hydrogen-bonding with the side chain of Asn704.

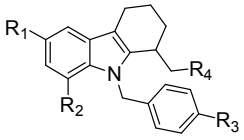

Compound	R_1	R_2	R_3	R_4	PDE2 IC_{50} (nM)
19	F	SO_2Me	CN	CO_2H	2801
20	F	SO_2Me	^iPr	CO_2H	61
21	F	SO_2Me	H	CO_2H	6526
22	F	SO_2Me	CF_3	CO_2H	41
23	F	CF3	CF_3	CO_2H	233
24	F	CN	CF_3	CO_2H	422
25	F	Br	Cl	CO_2H	6100
26	H	SO_2Me	Cl	CO_2H	4850
27	F	SO_2Me	Cl	CO_2H	431
28	F	SO_2Me	Cl	$C(O)NH_2$	66879
29	F	SO_2Me	CF_3	CN	>278000

Table 1. SAR in tetrahydrocarbazole series.

Having obtained the structure of compound **11** bound in the PDE2 active site we were now able to better rationalize some of the SAR apparent in the series using racemic **22** as the base comparator. First, the co-crystallographic structure revealed the *N*-benzyl substituent as occupying the induced-fit selectivity pocket similar to the BAY60-7550 and TAK-915 co-crystallographic structures. SAR was consistent with this finding as hydrophobic para-substituents were tolerated as seen with compounds **20**, whereas the slightly more polarized nitrile substituent **19** displayed ~ 70-fold loss in potency, as did the fully unsubstituted phenyl ring **21**. The dramatic loss of activity for **21** most likely results from not fully occupying the lipophilic pocket resulting in either a trapped water molecule at the base of the lipophilic pocket or an unfilled void space between the base of the lipophilic pocket and the inhibitor as either case would contribute to an entropic penalty upon binding. As for the methylsulfone at the R2 position involved with a hydrogen-bonding interaction with Gln812, replacement with a trifluoromethyl (**23**) or a nitrile group (**24**) was surprisingly well tolerated. However replacement of the sulfone with a bromide (**25**) led to a deleterious 150-fold loss in PDE2 potency. As noted previously, the fluorine atom in compound **11** in the co-crystallographic structure appeared to be involved in a hydrogen-bonding interaction with conserved glutamine 859. The importance of this interaction on PDE2 potency is apparent when comparing compound **27** with compound **26** where the fluorine is replaced with hydrogen; this modification leads to a 10-fold drop in PDE2 potency. Lastly, the acetic acid group displays a number of water-mediated hydrogen-bonding interactions critical for PDE2 potency and a severe or total loss of activity is

affected when the acid functionality is replaced with either an amide as in compound **28** or a nitrile as in compound **29**.

In summary, HTS efforts identified a unique PDE2 inhibitor series. The hit compound **1** was optimized to give compound **4** with improved PDE2 activity and off-target selectivity. Compound **4** improved cognitive performance in a rodent novel object recognition task as well as a non-human primate object retrieval task. Co-crystallization studies of compound **11** in the PDE2 active site revealed unique binding interactions affording high PDE isoform selectivity.

Acknowledgements: Data were collected at Southeast Regional Collaborative Access Team (SER-CAT) 22-ID (or 22-BM) beamline at the Advanced Photon Source, Argonne National Laboratory. Supporting institutions may be found at www.ser-cat.org/members.html.
Use of the Advanced Photon Source was supported by the U. S. Department of Energy, Office of Science, Office of Basic Energy Sciences, under Contract No. W-31-109-Eng-38.

References and notes:

1. Harvey, P. D.; Strassnig, M. *World Psychiatry* **2012**, *11*, 73-79.
2. Boess, F. G.; Hendrix, M.; van der Staay, F.-J.; Erb, C.; Schreiber, R.; van Staveren, W.; de Vente, J.; Prickaerts, J.; Blokland, A.; Koenig, G. *Neuropharmacology* **2004**, *47*, 1081-1092.
3. Beaulieu, C.; Guay, D.; Wang, Z.; Leblanc, Y.; Roy, P.; Dufresne, C.; Zamboni, R.; Berthelette, C.; Day, S.; Tsou, N.; Denis, D.; Greig, G.; Mathieu, M.-C.; O'Neill, G. *Bioorg. Med. Chem. Lett.* **2008**, *18*, 2696.
4. Sturino, C. F.; O'Neill, G.; Lachance, N.; Boyd, M.; Berthelette, C.; Labelle, M.; Li, L.; Roy, B.; Scheigetz, J.; Tsou, N.; Aubin, Y.; Bateman, K. P.; Chauret, N.; Day, S. H.; Lvesque, J.-F.; Seto, C.; Silva, J. H.; Trimble, L. A.; Carriere, M.-C.; Denis, D.; Greig, G.; Kargman, S.; Lamontagne, S.; Mathieu, M.-C.; Sawyer, N.; Slipetz, D.; Abraham, W. M.; Jones, T.; McAuliffe, M.; Piechuta, H.; Nicoll-Griffith, D. A.; Wang, Z.; Zamboni, R.; Young, R. N.; Metters, K. M *J. Med. Chem.* **2007**, *50*, 794-806.
5. Baldi, E.; Bucherelli, C. *Nonlinearity Biol. Toxicol. Med.* **2005**, *3*, 9-21.
6. Eddins, D.; Hamill, T, G.; Puri, V.; Cannon, C. E.; Vivian, J. A.; Sanabria-Bohorquez, S. M.; Cook, J. J.;Morrow, J. A.; Thompson, F.; Uslaner, J. M. *Psychopharmacology* **2014**, *231*, 511-519.
7.Uslaner, J. M.; Eddins, D.; Puri, V.; Cannon, C. E.; Sutcliffe, J.; Chew, C. S.; Pearson, M.; Vivian, J. A.; Chang, R. K.; Ray, W. J.; Kuduk, S. D.; Wittmann, M. *Psychopharmacology* **2012**, *225*, 21-30.
8. Wang, Z.; Dufresne, C.; Guay, D.; Leblanc, Y. WO 200209483, 2002.
9. Corey, E. J.; Helal, C. J. *Ang. Chem. Int. Ed.* **1998**, *37*, 1986-2012.
10. Li, L.; Beaulieu, C.; Carriere, M.-D.; Denis, D.; Greig, G.; Guay, D.; O'Neill, G.; Zamboni, R.; Wang, Z. *Bioorg. Med. Chem. Lett.* **2010**, *20*, 7462-7465.
11. Beaulieu, C.; Guay, D.; Wang, Z.; Zamboni, R. WO2005056527, 2005.
12. Structural coordinates have been deposited in the PDB: code 6BLF
13. Zhu, J.; Yang, Q.; Dai, D.; Huang, Q. *J. Am. Chem. Soc.* **2013**, 135, 11708-11711.

Graphical Abstract

An internal HTS effort identified a novel PDE2 inhibitor series that was subsequently optimized for improved PDE2 activity and off-target selectivity. The optimized lead, compound **4**, improved cognitive performance in a rodent novel object recognition task as well as a non-human primate object retrieval task. In addition, co-crystallization studies of close analog of 4 in the PDE2 active site revealed unique binding interactions influencing the high PDE isoform selectivity.

Rhesus Object Retrieval

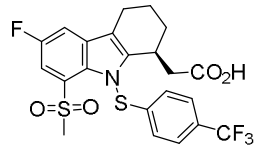

4

PDE2 IC_{50} = 5 nM